Comparison of the Fouling Release Properties of Hydrophobic Fluorinated and Hydrophilic PEGylated Block Copolymer Surfaces: Attachment Strength of the Diatom *Navicula* and the Green Alga *Ulva*

Sitaraman Krishnan,[†] Nick Wang,[†] Christopher K. Ober,*,[†] John A. Finlay,[‡]
Maureen E. Callow,[‡] James A. Callow,[‡] Alexander Hexemer,[§] Karen E. Sohn,[§]
Edward J. Kramer,[‖] and Daniel A. Fischer[⊥]

Department of Materials Science and Engineering, Cornell University, Ithaca, New York 14853, School of Biosciences, The University of Birmingham, Edgbaston, Birmingham B15 5TT, U.K., Department of Materials, University of California at Santa Barbara, Santa Barbara, California 93106, and National Institute for Standards and Technology, Gaithersburg, Maryland 20899

To understand the role of surface wettability in adhesion of cells, the attachment of two different marine algae was studied on hydrophobic and hydrophilic polymer surfaces. Adhesion of cells of the diatom *Navicula* and sporelings (young plants) of the green macroalga *Ulva* to an underwater surface is mainly by interactions between the surface and the adhesive exopolymers, which the cells secrete upon settlement and during subsequent colonization and growth. Two types of block copolymers, one with poly(ethylene glycol) side-chains and the other with liquid crystalline, fluorinated side-chains, were used to prepare the hydrophilic and hydrophobic surfaces, respectively. The formation of a liquid crystalline smectic phase in the latter inhibited molecular reorganization at the surface, which is generally an issue when a highly hydrophobic surface is in contact with water. The adhesion strength was assessed by the fraction of settled cells (*Navicula*) or biomass (*Ulva*) that detached from the surface in a water flow channel with a wall shear stress of 53 Pa. The two species exhibited opposite adhesion behavior on the same sets of surfaces. While *Navicula* cells released more easily from hydrophilic surfaces, *Ulva* sporelings showed higher removal from hydrophobic surfaces. This highlights the importance of differences in cell−surface interactions in determining the strength of adhesion of cells to substrates.

1. Introduction

Whether cells adhere strongly to hydrophobic or hydrophilic polymer surfaces is a question that has relevance in several areas of science and technology including design of materials for medical implants, biosensors, or antifouling surfaces. Many cells secrete adhesive macromolecules to enhance or enable attachment to surfaces.[1] The strength of adhesion is influenced by wetting of the underwater surface by the adhesive matrix.[2] Wetting refers to the phenomenon of spreading of a liquid on a substrate and is controlled by molecular interactions of the liquid (adhesive matrix in the case of cell adhesion) with the surface, quantified by surface energy.[3] Low-energy surfaces, in general, are difficult to wet.[3] In the area of marine biofouling, low-surface-energy poly(dimethyl siloxane) (PDMS) elastomers are used commercially as "fouling release" coatings, so-called because fouling organisms adhere only weakly and are "released" under suitable hydrodynamic conditions.[4−6] Although macrofoulers such as barnacles are released from silicone-based elastomers under suitable water shear stress, slimes dominated by diatoms persist.[7] One of the challenges in the area of marine

coatings technology is to develop a coating that will resist strong adhesion of all forms of biofouling,[8] including diatoms.

More than three decades ago, Baier proposed that a critical surface energy in the range 20−30 mJ/m^2 imparted resistance to cell adhesion−not only to medical implants in contact with blood, where the weakly adhered platelets would be removed by interfacial shear forces generated by blood flow, but also in the prevention of marine fouling.[9,10] The adhesion of a number of bacteria was also shown to conform to what is now known as the "Baier curve".[11] Andrade et al., on the other hand, have postulated that surfaces such as those of hydrogels, with the lowest interfacial energy (not surface energy), will be highly resistant to platelet adhesion.[12] Poly(ethylene glycol) (PEG)-coated surfaces, with a relatively high surface energy (∼43 mJ/m^2),[13] but low interfacial energy with water, are now well-known to be resistant to cell adhesion,[14−16] possibly due to the steric repulsion of the adhesive molecule caused by the hydrated PEG chains.[17] There are an increasing number of reports that surface or interfacial energy is not the sole factor affecting bioadhesion. Surface energy quantifies molecular interactions at equilibrium. Polymeric surfaces, however, are capable of undergoing molecular reorganization depending on their environment. Surface reconstruction,[18−20] surface roughness,[21−23] the chemical nature of cell exopolymers, mechanical properties of the surface,[24−28] the nature of the adhering cell and the extracellular matrix,[29,30] duration of contact of the cell with the surface,[31] and the presence of a conditioning film on the surface[17,32−35] are all expected to influence the attachment strength of cells to surfaces.

* To whom correspondence should be sent. E-mail: cober@ccmr.cornell.edu. Tel 607-255-8417; Fax 607-255-2365.

† Cornell University.

‡ The University of Birmingham.

§ Department of Materials, University of California at Santa Barbara.

‖ Department of Materials and Department of Chemical Engineering, University of California at Santa Barbara.

⊥ National Institute for Standards and Technology.

In this paper, we examine adhesion of two marine algae to well-characterized hydrophobic and hydrophilic polymer surfaces, with the goal of developing improved environmentally benign surfaces for marine antifouling applications. The test algae represent two key groups of fouling organisms, namely, micro- and macrofouling, and were specifically chosen because they have contrasting mechanisms of adhesion. In the following paragraphs, we describe these organisms and their adhesion mechanisms.

1.1. Adhesion of Diatoms and *Ulva* Sporelings. Slimes dominated by diatoms are the predominant form of microfouling on marine surfaces including both biocidal and nonbiocidal coatings.[36,37] Diatoms are unicellular algae characterized by the presence of an elaborately ornamented silica cell wall known as the frustule. Raphid diatoms are those that possess a raphe(s), which is a slit in the frustule allowing secretion of sticky extracellular polymeric substances (EPS) for both adhesion and motility.[37-39] The EPS is a multicomponent, mucilaginous, organic bioadhesive, mainly composed of acidic polysaccharides[40] and proteoglycans.[41] Although diatoms can glide once attached to a surface, providing EPS is continuously produced,[38] they are not motile in the water column and reach a surface either by gravity or in water currents.

The adhesion biology of *Ulva* (syn. *Enteromorpha*) is quite different from that of diatoms. Dispersal is mainly through asexual zoospores: quadriflagellate, pear-shaped cells, 5−7 μm in length. Colonization of substrata involves the transition from a free-swimming spore to an adhered nonmotile spore,[42] adhesion being achieved via the exocytotic secretion of a hydrophilic glycoprotein adhesive present in swimming spores.[42-44] Cross-linking of the adhesive,[45] with a corresponding increase in adhesion strength[31] and modulus,[30] begins immediately after settlement. The spore germinates to form a multicellular sporeling (young plant), which after one week of growth is approximately 100 μm in length. Adhesion of sporelings to the substratum is mediated by the glycoprotein spore adhesive, which continues to be formed following cell division, along with other sticky polymers that are secreted by the rhizoids ("rootlets") that are in contact with the substratum.[37,46,47]

2. Motivation

Brady has proposed that the empirical Baier curve, relating the adhesion strength to surface energy, has its basis in the mechanics of fracture at the interface of the cell adhesive and the substrate.[8] The stress required to detach a microorganism from the coating is given by $(WE_c/a)^{1/2}$ where W is the work of adhesion or the energy per unit area needed to separate the interface, a is the radius of the contact region, and E_c is the composite modulus of the adhesive matrix and the coating.[27] PDMS elastomers possess the properties required for fouling release, namely, a relatively low surface energy (ca. 22 mJ/m^2) that lies in the minimally adhesive region of the Baier curve and low modulus (3−1.4 MPa).[8,24,48] Yet, diatom slimes adhere more strongly to PDMS elastomers[49] and other hydrophobic surfaces than to hydrophilic surfaces.[50] Surfaces of hydrophobic fluorinated polymers have not been extensively studied for adhesion of diatoms or other foulers. Youngblood et al. found that fluorinated surfaces showed a high removal of settled zoospores of *Ulva*.[51] Contrary to the expectation that protein-resistant PEGylated surfaces should also resist cell adhesion, the adhesion of *Ulva* zoospores was found to be stronger on the PEGylated surfaces than the fluorinated surfaces. The
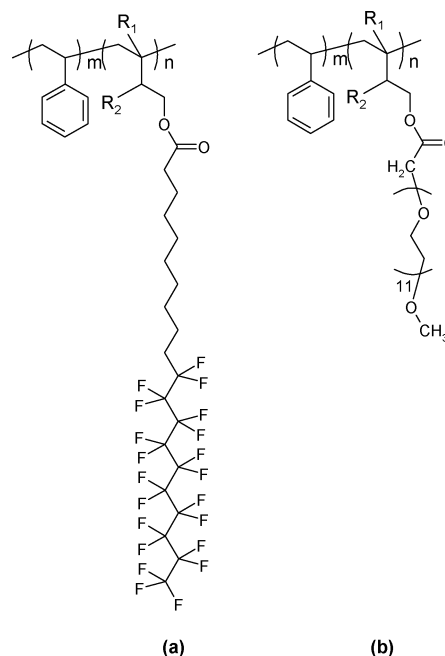

Figure 1. Comblike block copolymers with hydrophobic semifluorinated and hydrophilic PEG side-chains; R_1 = H (or CH$_3$) and R_2 = CH$_3$ (or H).

relative strengths of attachment of diatoms to hydrophobic fluorinated and hydrophilic PEGylated surfaces are not known. Moreover, Becker[52] has reported that the diatom *Amphora* shows a stronger adhesion to hydrophilic substrates (polycarbonate and glass) compared to hydrophobic fluorinated polymers,[53] which is not in accord with recent findings.[49,50] To resolve these issues, we studied adhesion of the diatom *Navicula perminuta* and sporelings of *Ulva linza* on surfaces of block copolymers shown in Figure 1. A special attribute of polymers with semifluorinated liquid crystalline side-chains is to resist surface reconstruction in a polar environment, which ensures that the surface remains nonpolar even after immersion in water.[54] The fluorinated surfaces had critical surface energy of about 8 mJ/m^2,[54] significantly lower than PDMS, while the PEGylated surfaces were expected to have a relatively low interfacial energy when in contact with water. This paper presents a comparison of the adhesion behavior of *Navicula* cells and *Ulva* sporelings on hydrophobic fluorinated and hydrophilic PEGylated surfaces.

2.1. Side-Chain Liquid Crystalline Fluorinated Polymers. Fluoropolymers are well-known for their nonpolar nature, which confers a low surface energy and a hydrophobic character to their surfaces.[55] However, polymers such as poly(tetrafluoroethylene) (PTFE) are completely insoluble in common organic solvents, have high crystallinity, melting temperature, and melt viscosity, and are difficult to bond to surfaces. These properties hinder their use as practical coatings on marine surfaces. In addition, because of its porous nature, marine adhesives invade the pores of PTFE and cross-link, resulting in a fairly strong adhesion of the organism by mechanical interlocking.[56] Polymers of fluorinated acrylates (or methacrylates), of the type CH$_2$=CH−COOR$_f$ where R$_f$ is a bulky fluoroalkyl group (e.g., −CF-(CF$_3$)$_2$), in contrast, are amorphous and have better solvent solubility.[57,58] The perfluoro isopropyl group also seems to effectively conceal the polar carbonyl group resulting in a critical surface energy of ca. 14 mJ/m^2, even lower than that of PTFE (ca. 18.5 mJ/m^2).[57] However, in the absence of a crystalline phase, these polymers are expected to reconstruct after immersion in water, exposing the more polar ester groups at the
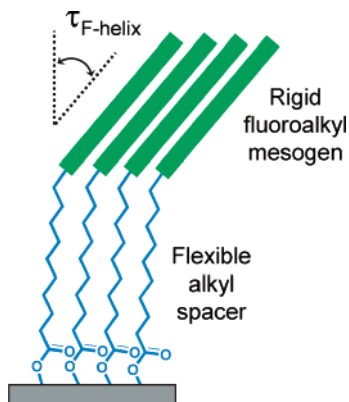
Figure 2. Liquid crystalline self-assembly of the semifluorinated side-chains to form a nonreconstructing hydrophobic surface under water. $\tau_{F-helix}$ is the angle made by the fluoroalkyl helix with the surface normal. The surface consists of different domains, in each of which the fluoroalkyl helices are oriented at an average angle of $\langle\tau_{F-helix}\rangle$. There is, however, no net azimuthal orientation. The average orientation of the fluorinated helices with respect to the surface normal can be determined by NEXAFS spectroscopy[60] or surface IR spectroscopy.[61]

polymer−water interface.[20] Wang et al. have shown that the block copolymer shown in Figure 1a forms a stable, nonreconstructing surface.[54] The fluoroalkyl group with a rigid, rodlike conformation is liquid crystalline (LC) in nature[59] and is connected to the polymer backbone via a flexible alkyl spacer that assists in LC assembly of the side-chains (cf. Figure 2).

Such block copolymers with semifluorinated liquid crystalline side-chains combine the advantages of the amorphous nature of the hydrocarbon part, imparting solubility, and the LC nature of the fluorocarbon part, imparting surface stability. A fairly long fluoroalkyl segment was chosen on the basis of the observation of Wang et al. that the thermal stability of the liquid crystalline phase increased significantly with every additional −CF_2− group in the side-chain.[55] Similarly, a long hydrocarbon segment was selected to compensate for the loss of solubility due to the fluorocarbon content. The formation of a smectic phase of the semifluorinated side-chains at the surface, with the mesogens oriented more or less normal to the surface, will result in a high density of −CF_3 groups and a highly nonpolar surface. Moreover, the long fluoroalkyl segment is expected to shield the uncompensated dipole at the −CH_2−CF_2− junction and also the polar ester group.

2.2. PEGylated Block Copolymers. The correlation between cell adhesion and protein adsorption on a surface is fairly complex.[14] Nevertheless, factors that are known to impart resistance to protein adsorption were considered while designing the PEGylated polymers that would be resistant to cell adhesion. Prime and Whitesides have shown that densely packed self-assembled monolayers of PEG with only a few ethylene oxide units per molecule, n (between 1 and 17), were resistant to protein adsorption.[62] However, the threshold grafting density (minimum number of PEG molecules per unit area of the surface) required for resistance to protein adsorption decreased with an increase in the PEG chain length. Andruzzi et al. also confirmed that densely grafted PEGylated polymer brushes with only 3 ethylene oxide units per monomer showed strong resistance to both protein adsorption and mast cell adhesion.[15] PEG with a molecular weight of ca. 550 g/mol ($n \approx 12$) was chosen to prepare the block copolymer with PEGylated side-chains (cf. Figure 1b). For relatively long oligo(ethylene glycol) chains ($n > 6$), protein resistance is not expected to depend on electrolyte concentration of the medium,[63] and antifouling

properties would be exhibited even in the marine environment. Moreover, on the basis of a study by Masuda and Nakanishi using several monovalent and divalent ions, only sulfate ions seem to have a strong de-swelling or "salting-out" effect on PEG gels in water.[64] But, the concentration of SO_4^{2-} ions in seawater is fairly low (∼0.03 mol/L at 3.5% salinity), so that salting-out is not expected to be an issue.

The surface-active block copolymers (SABCs) were synthesized by polymer analogous reactions on polystyrene-*block*-polyisoprene (PS-*b*-PI) precursors obtained by anionic polymerization. When the polymer surface is predominantly occupied by the surface-active PEGylated block, a high density of attachment of the PEG chains to the polymer backbone would also result in a high grafting density of PEG on the surface. The presence of the PS block of a sufficiently high molecular weight ensured that the PEGylated polymer did not dissolve away when the surface was immersed in water. A preferential segregation of the PS block to the surface is expected because of the slightly lower surface energy of PS (39.3 mJ/m^2)[13] compared to PEG (43 mJ/m^2)[13] when the surface is in contact with air, but this tendency would be reversed upon immersion in water. This is discussed further in the section on NEXAFS spectroscopy.

3. Experimental Methods

The experimental procedures, including the synthesis and characterization of the block copolymers, are discussed in detail in section 6. Here, we give an overview of the preparation of surfaces and the biofouling assays. Test surfaces were prepared on 3 in × 1 in glass microscope slides. As reported previously,[51] polystyrene-*block*-poly-(ethylene-*ran*-butylene)-*block*-polystyrene (SEBS) was used as a bottom primer layer, and the SABCs, coated on top of SEBS, were used to control the surface energy. In addition to imparting desired solubility characteristics to the surface-active polymer,[65] the polystyrene block improves polymer compatibility at the interface of SEBS and SABC by anchoring the PS block of SABC in the cylindrical PS domains of SEBS (cf. Figure 3). The bilayer approach also obviates the problem of poor bonding of fluorinated polymers to inorganic substrates. Methods for covalently bonding SEBS monolayers to silicon surfaces are well-known,[66,67] which we found to also effectively bind thicker SEBS films to glass. The surface-active block copolymers were applied by a spray-coating technique. Blending the fluorinated block copolymers with a small amount of SEBS was found to improve the roughness characteristics and wetting properties of the spray-coated surfaces. Thermal annealing at 120 °C for 12 h followed by a slow cooling to room temperature ensured surface enrichment of the low-surface-energy fluorinated block and the formation of a well-ordered smectic phase of the side-chains. All the surfaces were dried at 60 °C in a vacuum oven for 2 days, prior to the annealing step. The PEGylated surfaces, however, were not annealed after drying, as annealing was found to result in a surface rich in polystyrene.

The surfaces were characterized using dynamic water contact angle measurements, X-ray photoelectron spectroscopy (XPS) and near-edge X-ray absorption fine structure (NEXAFS) spectroscopy for chemical composition and molecular orientation, and optical interferometry and scanning force microscopy (SFM) for surface roughness.

Bioadhesion assays were performed using the marine diatom *Navicula perminuta*, which is ca. 10−15 μm long and ca. 5 μm wide.[49] The sticky EPS extruded through the raphes attaches the cells to the surface within ca. 2 h of settlement.[49] The surfaces were also tested for adhesion of *Ulva* sporelings cultured on the test surfaces. The strength of attachment of cells of *Navicula* and *Ulva* sporelings on different surfaces was compared by determining the average number of cells (*Navicula*) or biomass (*Ulva*) remaining attached to a surface after exposure to turbulent flow in a flow channel at 53 Pa wall shear
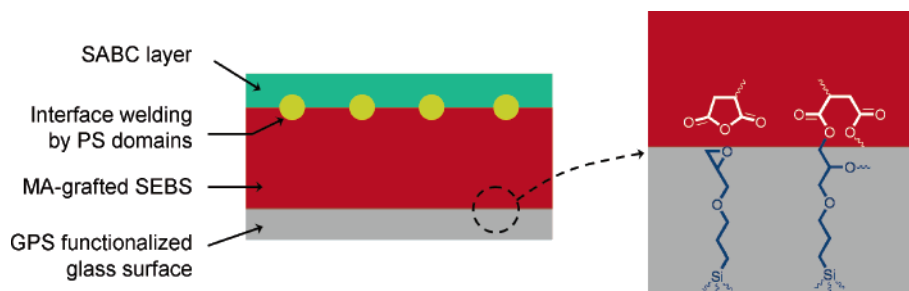
Figure 3. Schematic of bilayer coatings on 3-(glycidoxypropyl)trimethoxy silane (GPS)-functionalized glass slides (cross-sectional view, not to scale). The PS domains at the interface of the SABC and the SEBS bond the two polymer layers. Adhesion to glass is achieved by reaction between the epoxy groups on the glass surface and maleic anhydride (MA) groups of the MA-grafted SEBS.

Table 1. Advancing and Receding Water Contact Angles of Bilayer Coatings on Glass Microscope Slides, Prepared by Spray-Coating Technique

	water contact angles (deg)	
	advancing	receding
(27/13)F10H9	120 ± 2	82 ± 2
(10/12)F10H9	124 ± 2	87 ± 2
(27/13)PEG550	78 ± 2	25 ± 2
SEBS[a]	104 ± 1	69 ± 1
PDMS[b]	115 ± 4	69 ± 2

[a] Prepared by spin-coating a 1.5% (w/v) solution of SEBS in toluene on silicon wafer and annealing at 120 °C for 12 h. [b] As reported in ref 23.

stress. A fouling release silicone elastomer, Silastic T2 from Dow Corning, was included as a standard.

4. Results and Discussion

4.1. Sample Nomenclature. Block copolymers with the $F(CF_2)_{10}(CH_2)_9COO-$ side-chains (Figure 1a) are denoted by F10H9, while those with $CH_3O(CH_2CH_2O)_{11}CH_2COO-$ side-chains (Figure 1b) are denoted by PEG. The lengths of the two blocks are identified by the molecular weights of the PS and PI blocks in the precursors (in kg/mol). Thus, (27/13)F10H9 is the semifluorinated block copolymer prepared from PS-*b*-PI with PS and PI molecular weights of 27 and 13 kg/mol, respectively. The (27/13)F10H9 and (27/13)PEG550 block copolymers were prepared from the same PS-*b*-PI precursor, contained identical PS blocks, and had the same number of monomer units in the surface-active block. The (10/12)F10H9 and (27/13)F10H9 polymers had an almost identical surface-active block, but different lengths of the PS block.

4.2. Water Contact Angles and Surface Roughness. Table 1 shows the advancing angle, θ_a, and receding angle, θ_r, of a water drop on the three SABC surfaces that were used in the biofouling assays. Also included are the contact angles (CAs) on the SEBS and PDMS controls.

It is seen that all the surfaces showed a significant CA hysteresis ($\theta_a - \theta_r$), which may seem to indicate surface reconstruction.[18] However, we have observed that surface roughness was an important factor that contributed to the CA hysteresis.[72] A spin-coated surface of (10/12)F10H9 on a silicon wafer, annealed at 150 °C for 12 h to achieve fairly low roughness (~5 nm rms), showed advancing and receding water contact angles of 124° and 109°, respectively. On the contrary, when the same surface was not annealed, so that the surface roughness was higher (~18 nm rms), the θ_a and θ_r values were 130° and 65°, respectively. The higher advancing CA of the unannealed surface is clearly a sign of pinning of the three phase contract by a local defect (surface roughness, and possibly
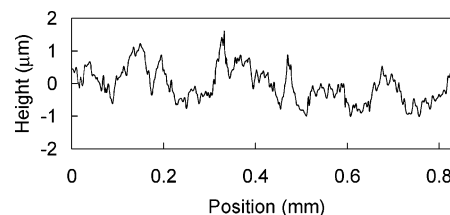

Figure 4. Line section of a representative optical interferometry image of a spray-coated (27/13)F10H9 bilayer coating on glass microscope slide. This microscale roughness is of significance in the study of interaction of organisms with sizes comparable to the peaks and valleys of the surface.

chemical heterogeneity[68]).[69] Surface reconstruction would require a disruption of the smectic layer of the semifluorinated mesogens (cf. Figure 2), which is not expected to readily occur at room temperature. We attribute the CA hysteresis to surface roughness and not surface reconstruction.[70] Figure 4 shows a representative topography of a (27/13)F10H9 surface on a glass substrate, determined by optical interferometry. The root-mean-square (rms) roughness of this surface (determined over a 0.65 mm × 0.85 mm region) was 0.9 ± 0.1 μm. The rms roughness of the spray-coated (10/12)F10H9 (with a lower molecular weight) was lower, 0.6 ± 0.1 μm, while that of the (27/13)-PEG550 surface was also 0.6 ± 0.1 μm.

With the PEGylated block copolymer, however, the observed difference in the two angles could also be due to surface penetration of water during CA determination.

4.3. NEXAFS Spectroscopy. Molecular composition and orientation in the top 3 nm of the surface was studied by NEXAFS spectroscopy. The spray-coated bilayer coatings of the (27/13)F10H9 and (10/12)F10H9 polymers indicated the presence of a smectic layer of oriented semifluorinated side-chains at the surface, similar to spin-coated thin films.[60,71,72] Figure 5 shows the C *K*-shell NEXAFS spectra of the (27/13)-F10H9 and (27/13)PEG550 surfaces. These spectra are quite distinct from those of PS and SEBS surfaces (also shown in the figure).

NEXAFS spectra of the fluorinated surfaces showed the characteristic 1s → σ^*_{C-F} resonance at ca. 293 eV, resulting from the fluoroalkyl segments in the side-chains. In addition, the normalized partial electron yield corresponding to this resonance was found to vary with the X-ray angle of incidence. In polarization-dependent X-ray absorption studies, the measured intensity is proportional to $\cos^2 \delta$ where δ is the angle between the transition dipole moment of the bond under consideration and the electric field vector, **E**, of the polarized X-ray beam.[74] Thus, the average tilt of C−F bonds at the surface could be determined by varying the angle of X-ray incidence and measuring the σ^*_{C-F} resonance intensity. Assuming that the perfluoroalkyl group forms a rigid helix with the C−F bonds
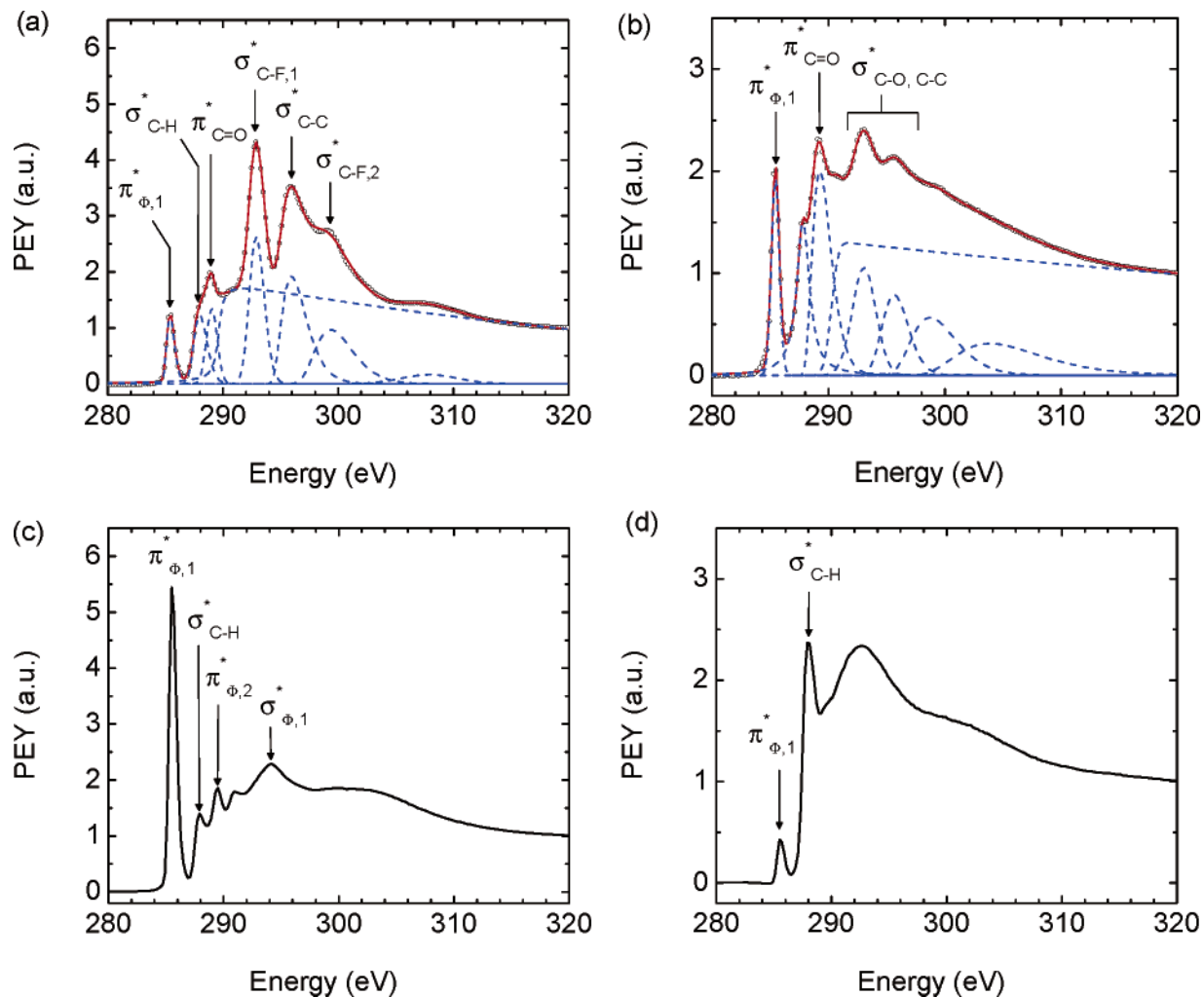
Figure 5. C *K*-shell NEXAFS spectra of (a) spray-coated (27/13)F10H9 bilayer coating on glass slide, (b) spray-coated (27/13)PEG550 bilayer coating on glass slide, (c) polystyrene, and (d) SEBS. All spectra were obtained using X-ray incidence angle of 55°. The peak assignments for PS are according to Stöhr (ref 73). The intensity of the $\pi^{*}_{\Phi,1}$ peak of the polystyrene surface is 5.44. The relative intensities of the $\pi^{*}_{\Phi,1}$ peaks in the block copolymer surfaces are proportional to the surface styrene contents.

normal to the axis of the helix, the average tilt, $\langle\tau_{\text{F-helix}}\rangle$, of the fluorinated helices (cf. Figure 2) could then be determined on the basis of the spinning chain model of Outka et al.[75] The ideal tilt angle of the helix is 0°, as it would result in a surface completely covered by the low-surface-energy $-CF_3$ groups. Both NEXAFS and IR spectroscopy have shown that the average tilt angle is higher as the lengths of the alkyl and fluoroalkyl segments are increased.[76] The experimental $\langle\tau_{\text{F-helix}}\rangle$ for the spray-coated F10H9 surfaces were found to be $(43 \pm 4)°$. A tilt angle greater than 0° might result in the exposure of some $-CF_2-$ groups,[77] but the fluoroalkyl segment is sufficiently long to mitigate the influence of underlying polar groups on the surface energy. The use of a blend of SABC with SEBS in the spray-coating formulation did not affect the surface composition or orientation of the side-chains. Using similar block copolymers with semifluorinated mesogens, Hexemer et al. found that a complete coverage of the surface with the fluorinated block could be achieved even when only about one-third of the polymer in the blend was the SABC, an effect attributed to the preferential segregation of the lower-surface-energy fluorinated block to the air–polymer interface.[71]

NEXAFS spectra of the (27/13)PEG550 surfaces indicated that the PEG side-chains were not oriented. This lack of orientation is a favorable aspect for antifouling properties, as surfaces comprising densely packed, nearly crystalline PEG

chains are not expected to resist protein adsorption.[62] In addition, the intensity of the $\pi^{*}_{\Phi,1}$ resonance, arising from the PS block, was higher for the (27/13)PEG surface (ca. 37% of that of pure PS) than the (27/13)F10H9 surface (ca. 22% of that of pure PS), indicative of a greater number of phenyl ring carbon atoms (cf. Figure 5a,b). The presence of both PEG and PS at the surface is due to comparable surface energies of dry PEG and PS. Because of the slightly higher surface energy of PEG, a preferential segregation of PS is expected in air or vacuum. Despite this, the presence of PEG side-chains at the surface is evident from the NEXAFS spectrum of Figure 5b,[78] from XPS (cf. section 4.4), and the water contact angle values. Thermal annealing was found to increase the surface content of the PS block (and the water contact angles). By drying the surface at a temperature below the glass transition temperature of PS, it was possible to lock the nonequilibrium surface composition that was relatively richer in the PEGylated block. Although the surface composition in air is expected to be highly dependent on processing conditions such as solvent, humidity, and temperature, the equilibrium surface, after immersion in water, will be rich in the PEGylated block.

Figure 6 compares the NEXAFS spectra of the (27/13)F10H9 and (10/12)F10H9 surfaces. The (27/13)F10H9 surface had a higher content of phenyl ring carbon atoms (from the PS block) and a lower content of $-CF_2-$ and $-CF_3$ carbon atoms (from
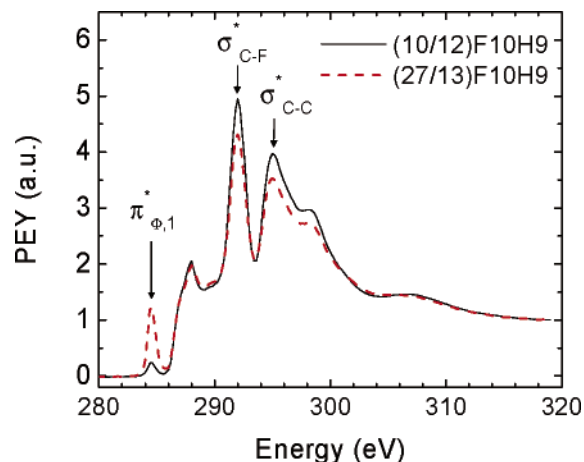
Figure 6. C *K*-shell NEXAFS spectra of spray-coated (27/13)F10H9 and (10/12)F10H9 bilayer coating on glass slides, obtained at X-ray incidence angle of 55°.

Table 2. Comparison of the Experimental Atomic Percentages of Carbon with Stoichiometric Values Assuming that Only the Fluorinated Blocks Were Present at the Surface

	atomic percent	
	experimental	stoichiometry
C—C, C=C	55	52
C—O	5	4
C=O	4	4
CF_2	32	36
CF_3	4	4

the side-chains of the fluorinated block). The normalized $\pi^*_{\Phi,1}$ peak intensities are 22% and 4%, respectively, of that of a pure PS surface. Apparently, the longer PS block of the (27/13)-F10H9 cannot reorganize sufficiently (by moving away from the surface and allowing the lower-energy fluorinated block to surface-segregate) without annealing at higher temperatures. However, the PS peaks in the NEXAFS spectra of both polymers were found to almost disappear upon prolonged annealing (120 °C for 24 h). A goal, toward the construction of a highly nonpolar surface, is to minimize the presence of the higher-surface-energy styrene units, and hence lower the NEXAFS $\pi^*_{\Phi,1}$ resonance. As will be seen in the section of *Ulva* bioassay, the presence of PS at the surface of the fluorinated block copolymer was found to result in inferior fouling release properties.

4.4. X-ray Photoelectron Spectroscopy. Figure 7 shows high-resolution carbon 1s XPS spectra, for electron emission along the surface normal, obtained from the (27/13)F10H9 and (27/13)PEG550 surfaces. The subpeaks were resolved by curve-fitting as shown in the figure. The fluorinated surface showed distinct —CF_2— and —CF_3 peaks at binding energies near 291.3 and 293.5 eV, respectively (cf. Figure 7a). Table 2 compares the atomic percentages of carbon atoms in different functional groups to what would be expected if only the fluorinated block

were present at the surface and of uniform composition in depth. The experimental values were determined on the assumption that the photoionization cross-section of a carbon atom is independent of chemical environment. The good agreement between the two sets of values indicates that the surface was predominantly covered by the lower-surface-energy fluorinated block. The (27/13)PEG550 surface showed the expected C—C peak near 285 eV, the C—O—C peak near 286.5 eV, the C=O peak near 289 eV, and a phenyl ring shake-up peak just below 292 eV. The presence of the shake-up peak confirms the results of NEXAFS (Figure 5b), which showed that considerable PS was present near the surface. Given that a minor amount of phenyl groups were also seen near the (27/13)F10H9 surface, in the NEXAFS spectrum of Figure 5a, there must also be a phenyl ring shake-up peak for this sample, but it could not be separated from the —CF_2— peak. The good agreement shown in Table 2 suggests this shake-up peak cannot be very large.

4.5. *Navicula* Settlement and Detachment. The surfaces were incubated with cells in the logarithmic phase of growth for 2 h in the light. The settlement density of cells on all the surfaces was found to be similar ($\sim$750 cells/mm^2). This is not surprising, since diatom cells are nonmotile, and they rapidly fall in the water column and make contact with the surface. Thus, at the end of the 2 h incubation period, all substrates had a similar number of cells in contact with the surface. The strengths of attachment, determined using the turbulent flow channel, are shown in Figure 8. One-way ANOVA followed by a Tukey test showed significant differences in attachment strengths to the various surfaces. Attachment was the weakest (i.e., percentage removal was highest) on the hydrophilic PEGylated and glass surfaces. By contrast, the majority of cells remained attached to the hydrophobic (27/13)F10H9 and PDMS
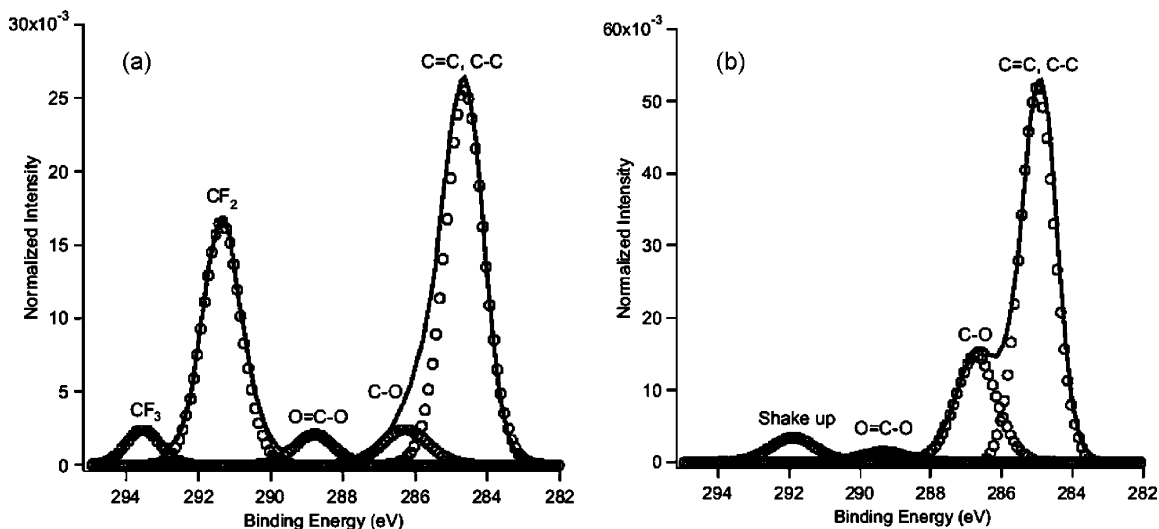

Figure 7. The XPS carbon 1s spectra of (a) (27/13)F10H9 surface and (b) (27/13)PEG550 surface. These spectra are normalized so that the total area under all the C 1s peaks is unity.
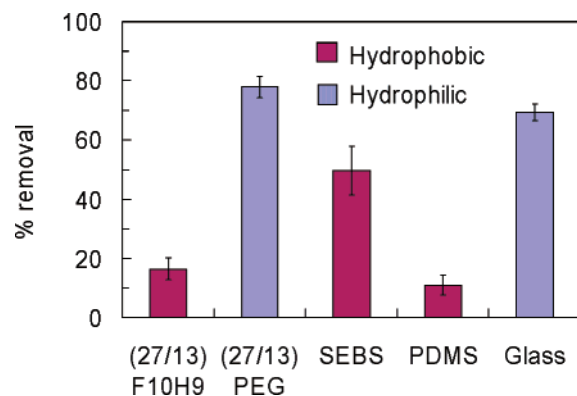
Figure 8. Percentage removal of *Navicula* from surfaces after exposure to water flow in a turbulent channel generating a wall shear stress of 53 Pa. Surfaces with advancing water contact angle, θ_a, greater than 90° are categorized as hydrophobic, while those with lower advancing water contact angles are called hydrophilic. Each point represents the mean percentage removal from 90 counts from 3 replicate slides. Bars represent 95% confidence limits derived from arcsine-transformed data.

Figure 9. (a) Growth of *Ulva* sporelings and (b) removal after exposure to shear stress of 53 Pa in the flow channel. Bars show the standard error of the mean derived from arcsine-transformed data from six replicate slides.

surfaces after exposure to 53 Pa wall shear stress. The percent removal from the (27/13)F10H9 and the PDMS surfaces were not significantly different, both being significantly lower than that from any of the other surfaces ($F_{4,385} = 216.5$, $p < 0.05$). SEBS, with mainly the poly(ethylene-*ran*-butylene) block at the surface,[79] showed a moderate removal of diatoms.

4.6. Detachment of *Ulva* Sporelings. Sporelings grew on all surfaces covering the slides with a green lawn after 8 days. One-way ANOVA ($F_{5,28} = 5.54$, $p < 0.05$) followed by a Tukey test showed significantly reduced growth on the (10/12)F10H9 and PEGylated surfaces compared with the PDMS or glass standards. There were no significant differences in growth between the fluorinated and PEGylated test surfaces. Percentage removal of sporelings is shown in Figure 9b. Removal from the two fluorinated surfaces was high, and one-way ANOVA ($F_{5,28} = 12.89$, $p < 0.05$) followed by a Tukey test showed that they were not significantly different from that of the PDMS standard. Both the (10/12)F10H9 surface and the PDMS standard showed a statistically significant higher removal compared to the PEGylated surface (at $p < 0.05$). Surfaces of glass, PEGylated block copolymer, or SEBS showed relatively low percentage removal values, which were not significantly different from each other.

5. Conclusion

Well-characterized, highly nonpolar, stable hydrophobic surfaces and polar hydrophilic surfaces were evaluated for strength of attachment of cells of the diatom *Navicula* and sporelings of *Ulva*. *Navicula* showed a stronger attachment to hydrophobic surfaces than to hydrophilic surfaces. The *Ulva* sporelings, however, showed an opposite behavior. Removal of sporelings was highest from the hydrophobic fluorinated and PDMS surfaces. The adhesion behavior of *Ulva* sporelings to elastomeric surfaces with different wetting characteristics agrees with that of zoospores, as reported previously by Youngblood et al.[51] The adhesive secreted by an *Ulva* spore spreads to a greater extent on a hydrophilic surface.[2] The larger area of contact of the adhesive pad and a lower contact angle of the adhesive matrix with the surface (resulting in a weak stress singularity at the contact line)[27] are believed to result in stronger attachment to hydrophilic surfaces. Why the adhesion of diatom cells should be so tenacious to nonpolar surfaces is not
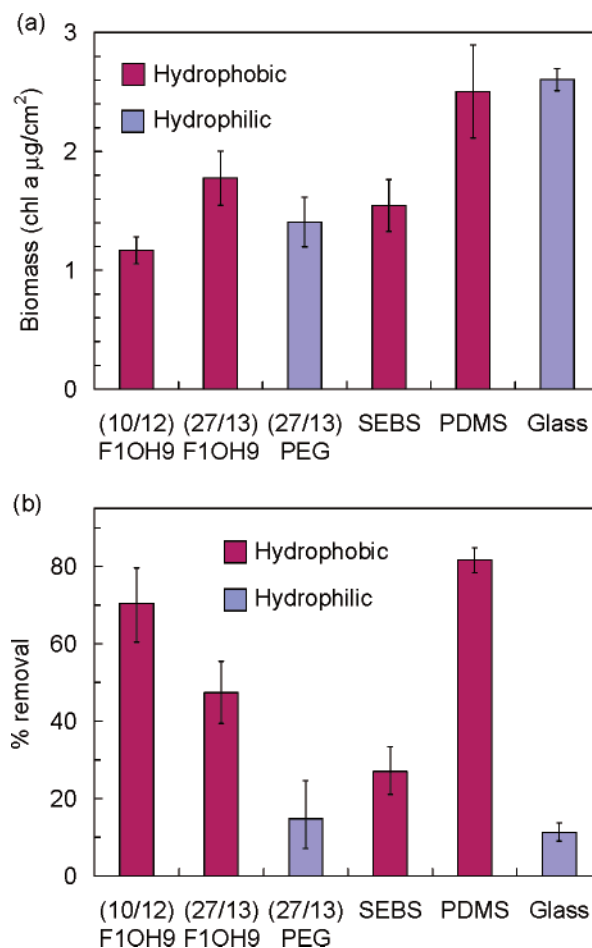
understood, but the answer presumably lies in the different physicochemical properties of their extracellular adhesives (see recent reviews in refs 80 and 81).

The dependence of adhesion strength on the properties of the adhesive liquids secreted by the organisms can be rationalized using the thermodynamic analysis of Dexter.[11] To explain the influence of surface wettability on bacterial attachment to surfaces, Dexter has proposed that bacterial settlement was determined by the rate of formation and composition of a "conditioning film" of organic molecules, which adsorbed on the surface within the first few minutes of immersion in water. However, his analysis would be valid even in the absence of a conditioning film, if the organic matter of the conditioning film is considered to be the EPS of the settling cells. Depending on the values of the interaction parameters, Φ_{sw}, Φ_{sp}, and Φ_{wp}, Dexter has shown that the Helmholtz free energy change for wetting of the solid surface, $\Delta F = \gamma_{sp} + \gamma_{pw} - \gamma_{sw}$, can decrease continuously, increase continuously, or pass through a maximum, when plotted against the critical surface tension, γ_{cs}, of the solid. The subscripts s, p, and w refer to the solid surface, EPS and water, respectively. The critical surface tension of the solid is defined such that $\gamma_p < \gamma_{cs}$ results in total wetting (the EPS, with a surface tension of γ_p, spreads completely on the solid) and $\gamma_p > \gamma_{cs}$ results in partial wetting (the EPS forms a spherical cap resting on the surface with a nonzero contact angle at equilibrium). The interaction parameter, which characterizes intermolecular forces between two surfaces in contact, is defined, for example, by $\gamma_{sw} = \gamma_s + \gamma_w - 2\Phi_{sw}(\gamma_s\gamma_w)^{1/2}$ in the case of

solid−water interface. Here, γ_s is the surface free energy of the solid in a vacuum, γ_w is the surface tension of water, and γ_{sw} is the solid−water interfacial energy. $\Phi = 1$ when the intermolecular forces at the interface are of the same type as those within both the contacting media. If ΔF versus γ_{cs} shows a maximum at a certain value of γ_{cs}, settlement would be the lowest on a solid with this value of critical surface tension, which is the basis of the empirical Baier curve. It is possible that, because of differences in Φ_{sp} values for EPS secreted by different organisms, ΔF increases (and hence settlement would be lower) with an increase in γ_{cs} for one organism, while ΔF decreases (and settlement would be higher) with an increase in γ_{cs}, for the other organism.

Experimentally, it is observed that settlement and adhesion strength of cells are not always correlated. A large number of cells may preferentially settle on a surface, but their adhesion could nevertheless be weak, as in the case of the *Ulva* zoospores.[50] The higher attachment strength of *Ulva* spores on a surface where its settlement is the lowest has been attributed, as discussed before, to the mechanics of fracture at the spore−surface interface.[27]

While there are suggestions in the literature that a surface energy below the minimally adhesive range of the Baier curve $(20-30 \text{ mJ/m}^2)$ may actually be counterproductive in preventing marine biofouling,[56,82] we find the low-surface-energy fluorinated polymers to show a fouling-release performance comparable to that of PDMS, suggesting that further effort on low-surface-energy fluoropolymer coatings should still be rewarding.

In conclusion, while the PEGylated block copolymer surfaces offer promise as antifouling coatings for diatom fouling, they are unlikely to be as effective in dealing with fouling by *Ulva* and other macrofouling organisms. On the contrary, the fluorinated block copolymer surfaces show good *Ulva* sporeling release, comparable to PDMS, but are ineffective against diatom fouling. Preference of surfaces with different wettabilities by different organisms has also been observed in the case of marine invertebrates. The settlement rates of bryozoan and ascidian larvae are higher, while those of barnacle cypris larvae are lower, on surfaces with lower wettability.[83] An important goal of marine antifouling research remains the identification of a surface that minimizes both the settlement density and the attachment strength of a variety of organisms. Amphiphilic surfaces, resulting from incorporation of both fluoroalkyl and PEG segments, have recently been found to be effective in controlling diatom as well as macroalgal fouling.[84] These types of surfaces may ultimately provide release to a much broader range of foulers.

6. Experimental Details

6.1. Materials and Methods. Styrene (CAS #100−42−5, FW 104.15, 99%) and isoprene (CAS #78−79−5, FW 68.12, 99%), stirred over dry di-*n*-butylmagnesium (received from Sigma-Aldrich as a 1.0 M solution in heptane) for 12 h and distilled after three freeze−thaw−degas cycles, were used to prepare polystyrene-*block*-polyisoprene (PS-*b*-PI) by anionic polymerization using *sec*-butyllithium (*s*-BuLi, CAS #598−30−1, CH$_3$CH$_2$CHLiCH$_3$, 1.4 M solution in cyclohexane) initiator.

9-Borabicyclo[3.3.1]-nonane (9-BBN, CAS #280−64−8, received as a 0.5 M 9-BBN solution in tetrahydrofuran), hydrogen peroxide solution (30 wt % in water), and sodium hydroxide (NaOH, CAS #1310−73−2, FW 40.00) were used for hydroxylation of the pendant vinyl groups of polyisoprene by the hydroboration−oxidation reaction. Perfluorodecyliodide (CAS #423−62−1, F(CF$_2$)$_{10}$I, FW 645.98), 9-decen-1-ol (CAS #13019−22−2, H$_2$C=CH(CH$_2$)$_8$OH, FW 156.27),

2,2′-azobisisobutyronitrile (CAS #78−67−1, N≡CC(CH$_3$)$_2$N=NC-(CH$_3$)$_2$C≡N, FW 164.21), and tributyltin hydride (CAS #688−73−3, (*n*-Bu)$_3$SnH, FW 291.06) were used to synthesize 10-perfluorodecyl-1-decanol (CAS #129794−52−1, F(CF$_2$)$_{10}$(CH$_2$)$_{10}$OH, FW 676.35), which was oxidized to 10-perfluorodecyl-1-decanoic acid (CAS #187867−25−0, F(CF$_2$)$_{10}$(CH$_2$)$_9$COOH, FW 690.33) using nitrogen dioxide (CAS #10544−72−6, ≥99.5%).
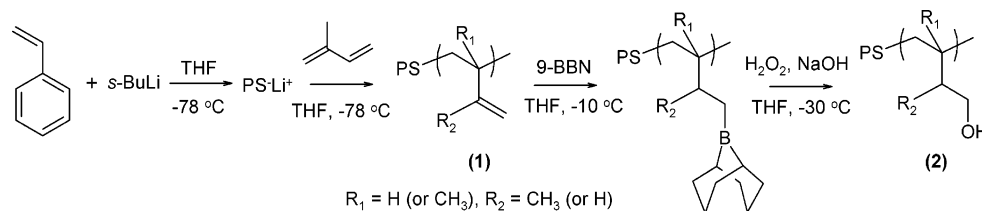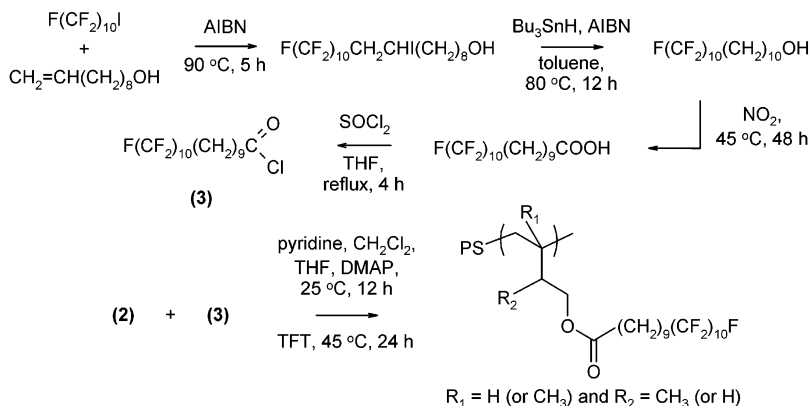
The terminal hydroxymethyl groups of poly(ethylene glycol) methyl ether (mPEG, CAS #9004−74−4, CH$_3$(OCH$_2$CH$_2$)$_x$OH, average $M_n \approx 550$, $x \approx 12$) were oxidized using trichloroisocyanuric acid (TCCA, CAS #87−90−1, FW 232.41), 2,2,6,6-tetramethyl-1-piperidinyloxy (TEMPO, CAS #2564−83−2, FW 156.25), sodium bromide (NaBr, CAS #7647−15−6, FW 102.89), sodium carbonate (Na$_2$CO$_3$, CAS #497−19−8, FW 105.99), and sodium bicarbonate (NaHCO$_3$, CAS #144−55−8, FW 84.01) to obtain mPEG ω-carboxylic acid, CH$_3$(OCH$_2$-CH$_2$)$_{x-1}$OCH$_2$COOH.

The semifluorinated or mPEG carboxylic acids were attached to the hydroxylated PI backbone after conversion to the corresponding acid chlorides using thionyl chloride (SOCl$_2$, CAS #7719−09−7, FW 118.97). The esterification was carried out using 1,3-dicyclohexylcarbodiimide (DCC, CAS #538−75−0, C$_6$H$_{11}$N=C=NC$_6$H$_{11}$, FW 206.33, 99%) and 4-(dimethylamino)pyridine (DMAP, CAS #1122−58−3, (CH$_3$)$_2$NC$_5$H$_4$N, FW 122.17, 99%) in appropriate mixtures of solvents, including anhydrous pyridine (99.8%), anhydrous dichloromethane (99.8%), anhydrous α,α,α-trifluorotoluene (TFT, CAS #98−08−8), and tetrahydrofuran (THF). THF was freshly distilled from Na/benzophenone, while all other solvents were used as received. All of the above chemicals were obtained from Sigma-Aldrich and used as received.

3-(Glycidoxypropyl)trimethoxysilane (GPS, CAS #2530−83−8) was purchased from Gelest. Polystyrene-*block*-poly(ethylene-*co*-butylene)-*block*-polystyrene (SEBS) triblock thermoplastic elastomer (KRATON G1652M), and SEBS grafted with maleic anhydride (MA−SEBS, KRATON FG1901X) were received from KRATON Polymers. Acetone (≥99.5%, Fisher), methanol, and toluene (technical grades, Fisher), 96% sulfuric acid, 95% ethanol, and all other reagents were used as received.

Gel permeation chromatography of THF solution of polymers (1 mg/mL) was carried out using four Waters Styragel HT columns operating at 40 °C and Waters 490 ultraviolet (254 nm wavelength) and Waters 410 refractive index detectors. The molecular weight range of the columns was from 500 to 10^7 g/mol. THF was used as the eluent at a flow rate of 1 mL/min, and toluene used as marker for flow calibration. The IR spectra of the polymers, cast as films from CHCl$_3$ solutions, on sodium chloride or potassium bromide salt plates were collected using a Mattson 2020 Galaxy Series FTIR spectrometer. ^{1}H and ^{13}C NMR spectra were recorded using Varian Gemini spectrometer with deuterated solvents. Differential scanning calorimetry was performed using a Perkin-Elmer DSC-7 instrument with a 10 °C/min heating and cooling rate.

6.2. Polymer Synthesis and Characterization. Block copolymers with semifluorinated side-chains were prepared using the procedure reported by Wang et al.[54] PS-*b*-PI (**1**) copolymers with high vinyl content (3,4- and 1,2- microstructures) were obtained by anionic polymerization using THF, a polar solvent, at −78 °C. The PI block was then hydroxylated using the hydroboration−oxidation reaction[85−87] where a 9-BBN adduct of isoprene is reacted with 3 equiv of the hydroperoxide anion, HOO$^-$ (formed by deprotonation of H$_2$O$_2$ in basic solution) to produce a trialkyl boronate ester, which undergoes base-catalyzed hydrolysis to give hydroxylated isoprene (Scheme 1) with cyclooctane-1,5-diol and boric acid[88] as side products. 10-Perfluorodecyl-1-decanol was prepared as described in Höpken et al.[89] Free-radical addition of perfluordecyl iodide to 9-decen-1-ol resulted in 9-iodo-10-perfluorodecyl-1-decanol, which was reduced, without isolation, using tributyltin hydride to obtain the semifluorinated alcohol (Scheme 2). The alcohol was oxidized to 10-perfluorodecyldecanoic acid with nitrogen dioxide.[54] Attachment to hydroxylated PS-*b*-PI was achieved after conversion of the semifluorinated acid to acid chloride using thionyl chloride.

Scheme 1. Synthesis of Hydoxylated Polystyrene-*block*-Polyisoprene Copolymer

$+$ *s*-BuLi $\xrightarrow[\text{-78 °C}]{\text{THF}}$ PS⁻Li⁺ $\xrightarrow[\text{THF, -78 °C}]{}$ PS $\xrightarrow[\text{THF, -10 °C}]{\text{9-BBN}}$ PS $\xrightarrow[\text{THF, -30 °C}]{\text{H}_2\text{O}_2, \text{NaOH}}$ PS

(1)

R₁ = H (or CH₃), R₂ = CH₃ (or H)

(2)

Scheme 2. Synthesis of BCs with Semifluorinated Side-Chains

$F(CF_2)_{10}I$
$+$
$CH_2=CH(CH_2)_8OH$
$\xrightarrow[\text{90 °C, 5 h}]{\text{AIBN}}$
$F(CF_2)_{10}CH_2CHI(CH_2)_8OH$
$\xrightarrow[\substack{\text{toluene,}\\\text{80 °C, 12 h}}]{\text{Bu}_3\text{SnH, AIBN}}$
$F(CF_2)_{10}(CH_2)_{10}OH$

$\xrightarrow[\substack{\text{NO}_2,\\\text{45 °C, 48 h}}]{}$

$F(CF_2)_{10}(CH_2)_9C\overset{O}{\underset{Cl}{}}$ $\xleftarrow[\substack{\text{THF,}\\\text{reflux, 4 h}}]{\text{SOCl}_2}$ $F(CF_2)_{10}(CH_2)_9COOH$

(3)

(2) + **(3)** $\xrightarrow[\text{TFT, 45 °C, 24 h}]{\substack{\text{pyridine, CH}_2\text{Cl}_2,\\\text{THF, DMAP,}\\\text{25 °C, 12 h}}}$

$O-(CH_2)_9(CF_2)_{10}F$

R₁ = H (or CH₃) and R₂ = CH₃ (or H)

Gel permeation chromatography (GPC) showed the molecular weight of the polystyrene block to be ca. 10 000 g/mol with a polydispersity index (PDI) of 1.04. The molecular weight of the polyisoprene block, determined by ¹H NMR from the ratio of the areas under the aromatic protons and the vinyl protons of isoprene, was ca. 12 500 g/mol. The polydispersity index of the PS-*b*-PI polymer, determined by GPC, was 1.08. Thus, the degrees of polymerization of the polystyrene and polyisoprene blocks were ca. 95 and 185, respectively. A high extent of esterification was confirmed by the disappearance of the O−H stretching vibrations at 3334 cm⁻¹ of the hydroxylated PS-*b*-PI precursor and appearance of ester C=O stretching vibrations at 1737 cm⁻¹ and C−F band between 1000 and 1400 cm⁻¹. Differential scanning calorimetry showed the liquid crystalline nature of the block copolymer. Two distinct first-order transitions were observed at 98 and 113 °C and, on the basis of previous studies,[54] attributed to smectic-B to smectic-A, and smectic-A to isotropic transitions, respectively. PS/PI-(27/13) with PS and PI block molecular weights of 27 000 and 13 000 g/mol, respectively, was similarly prepared and modified.

Synthesis of Carboxyl-PEG. Carboxyl-PEG is usually synthesized by carboxymethylation of PEG with α-haloacid or its esters,[90,91] or by direct oxidation of the terminal hydroxymethyl group of PEG using oxidizing agents such as CrO₃ and sulfuric acid.[92] We have used relatively mild oxidizing conditions guided by reports that strong oxidizing agents, e.g., permanganate, cause polyether chain degradation.[91] Other problems with Cr(VI) or KMnO₄-based oxidation of PEG have been discussed by Vigo et al.[93] Oxidation of primary alcohols to carboxylic acid using *N*-oxoammonium salt is a highly attractive, mild, and metal-free route that has been extensively studied.[94] The *N*-oxoammonium salt is usually generated in situ by using a catalytic amount of 2,2,6,6-tetramethylpiperidine-1-oxy radical (TEMPO) and a stoichiometric amount of an oxidant such as bleach (NaOCl)[95] or trichloroisocyanuric acid (TCCA).[96,97] We have adapted the reaction scheme for oxidation of alcohols to carboxylic acid reported by De Luca et al.[96] to synthesize mPEG with terminal carboxylic acid groups. The *N*-oxoammonium ion produced by the reaction of TEMPO with TCCA oxidizes the hydroxymethyl group of mPEG to aldehyde, which is further oxidized to carboxylic acid by the hypochlorite ion generated by NaBr-catalyzed hydrolysis of TCCA. 100 mL of saturated sodium bicarbonate solution (10.3% w/v, 1.23 M) was added to a solution of 16.5 g (30 mmol) of mPEG in 150 mL acetone. After cooling to 0 °C, 0.617 g (3 mmol) of NaBr and 0.312 g (2 mmol) TEMPO were added, followed by a slow addition of 16.269 g (70 mmol) of TCCA. The

reaction mixture was warmed to room temperature and stirred for ca. 24 h at room temperature, after which 10 mL of 2-propanol was added. After the stirring was stopped, a fine white solid settled down. The supernatant was decanted, mixed with Celite 545 filter aid (diatomaceous earth), and filtered. The clear, yellow filtrate was concentrated under vacuum to remove acetone and treated with 100 mL of 1 M Na₂CO₃ in water (10.6% w/v). This resulted in further precipitation of a white solid and a clear, colorless filtrate after filtration. The precipitate, consisting of isocyanuric acid, its tautomer, cyanuric acid, and their derivatives, was insoluble in chloroform. The aqueous phase was washed with ethyl acetate, acidified using 150 mL of 2 N HCl solution to convert the water-soluble mPEG carboxylate to mPEG carboxylic acid that could be extracted with chloroform. Solvent was evaporated from the chloroform solution to yield 15.5 g of viscous, colorless liquid after drying under vacuum (ca. 91.6% yield). Quantitative conversion was confirmed by the disappearance of the δ 2.9 signal in ¹H NMR and also disappearance of δ 61.3 and δ 72.2 signals and appearance of δ 171.8 signal in ¹³C NMR.

mPEG550, CH₃O(CH₂CH₂O)ₓH. ¹H NMR (300 MHz, CDCl₃, δ referenced to residual CHCl₃): 2.90 (br s, 1H, −O*H*); 3.27 (br s, 3H, −OC*H₃*); 3.54, 3.55, 3.56 (−OC*H₂*C*H₂*−). On the basis of the areas of −OC*H₃* protons and all the protons, *x* was found to be ca. 12. ¹³C NMR (75 MHz, CDCl₃, δ referenced to CDCl₃): 58.7 (−O*C*H₃), 61.3 (−*C*H₂*C*H₂OH), 70.0, 70.2 (−*C*H₂*C*H₂O−), 71.6 −*C*H₂OCH₃), 72.2 (−*C*H₂*C*H₂OH). IR (dry film) $\tilde{\nu}_{max}$(cm⁻¹): 3480 (O−H stretching), 2872 (C−H stretching), 1113, 1457 (C−H bending).

mPEG550-COOH, CH₃O(CH₂CH₂O)ₓ₋₁CH₂COOH. ¹H NMR (300 MHz, CDCl₃, δ referenced to residual CHCl₃): 3.31 (br s, 3H, −OC*H₃*); 3.58, 3.59 (s, −OC*H₂*C*H₂*−); 4.14 (t, 2H, −OC*H₂*COOH), 8.75 (br s, 1H, −COO*H*). ¹³C NMR (75 MHz, CDCl₃, δ referenced to CDCl₃): 58.5 (−O*C*H₃), 67.9 (−O*C*H₂COOH), 70.4 (−*C*H₂*C*H₂O−), 71.4 −*C*H₂OCH₃), 171.8 (*C*=O). IR (dry film) $\tilde{\nu}_{max}$(cm⁻¹): 2872 (C−H stretching), 1738 (C=O stretching, acid), 1113, 1455 (C−H bending).

Attachment of Carboxyl-PEG to Hydroxylated Polystyrene-block-Polyisoprene Block Copolymer. 1.5 g (2.6 mmol) mPEG550-COOH was reacted with 6 mL thionyl chloride for 4 h in 4 mL anhydrous THF under reflux, after which THF and SOCl₂ were removed under vacuum. To a solution of 0.5 g of PS/PI(27/13)OH (2.2 mmol OH) and 75 mg DMAP in 2 mL anhydrous pyridine was added the PEG carboxylic acid chloride solution in 4 mL anhydrous THF. After reaction at room temperature for 12 h, the mixture was heated and maintained at 40 °C for 24 h. A rubbery polymer was obtained after precipitation
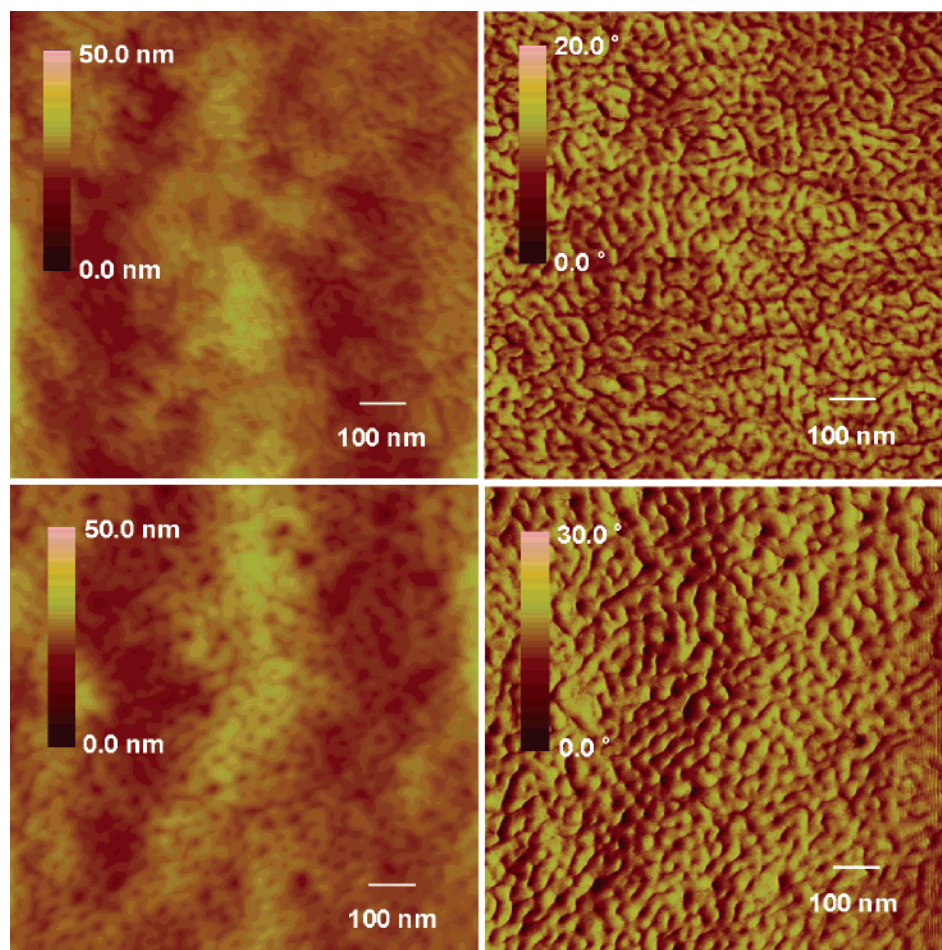
Figure 10. SFM topography (left) and phase (right) images of bilayer coatings on glass substrates prepared by spray-coating (top) and drop-casting (bottom) techniques. The rms roughness of the spray-coated surface (determined over a 2 μm × 2 μm region) was 73 nm, while that of the drop-cast surface was 44 nm. The advancing and receding water contact angles were 125° and 91°, respectively, on the drop-cast surface.

in water and drying under vacuum. IR (dry film) $\tilde{\nu}_{max}$(cm^{-1}): 2871 (C—H stretching, mPEG side-chains), 2917 (C—H stretching, polymer backbone), 1751 (C=O stretching, ester), 1113, 1455 (C—H bending), 700 (C—H bending, aromatic).

6.3. Surface Preparation and Characterization. The glass slides were cleaned in hot piranha solution (concentrated sulfuric acid + 30 wt % hydrogen peroxide solution, 7:3 v/v), rinsed with distilled water, and dried using nitrogen. A 2% (w/v) solution of (3-glycidoxypropyl)-trimethoxysilane in 95% ethanol (pH adjusted between 4.5 and 5 using acetic acid) was prepared by adding the silane to the ethanol solution and stirring for 5 min. The slides were then soaked in this solution for at least 1 h, rinsed with ethanol, and heated in an oven at 110 °C for 10 min. The GPS-functionalized glass slides were spin-coated with a toluene solution containing 5% (w/v) of MA-SEBS, and 2% (w/v) SEBS, and annealed in a vacuum-oven at 120 °C for 12 h. The styrene content of both SEBS and MA-SEBS was 30 wt %, and the latter had 1.4−2.0 wt % of grafted maleic anhydride. A noncatalyzed epoxy−anhydride curing mechanism[98] results in covalent attachment of SEBS to the glass surface. The surfaces were further spin-coated three times with 12% (w/v) solution of SEBS in toluene (2500 rpm) followed by vacuum-annealing at 120 °C for 12 h. 1.5% (w/v) solution of a blend of the fluorinated block copolymer (90 wt %) and SEBS (10 wt %) in 1:1 (v/v) TFT−toluene mixture was spray-coated on the SEBS surface using Badger model 250 airbrush (50 psi nitrogen gas pressure) to obtain a polymer surface density of 1.5−2 mg/cm^2. The PEGylated block copolymer was applied using a 1.5% (w/v) solution in 1:1 (v/v) THF−CH$_2$Cl$_2$ mixture. The surfaces were dried in a vacuum oven at 60 °C for 2 days, and the fluorinated surfaces were further annealed at 120 °C for 12 h. If the glass substrates were not functionalized with GPS

as described above, the coatings peeled off from the substrate in the flow channel, after immersion in seawater for a week.

Contact angles were measured using an NRL contact angle goniometer (Ramé-Hart model 100-00) at room temperature. Dynamic water contact angle measurements were performed by addition and retraction of a drop of water on the surface positioned on a stage that was checked for horizontal alignment using a spirit level.

Surface roughness was determined using a 3-D interferometric noncontact surface profiler (ADE Phase-Shift MicroAXM-100HR). Root-mean-square (rms) roughness values were determined over regions of 631 μm × 849 μm size and averaged over at least 10 measurements. The surface morphology was studied using Veeco Dimension 3100 scanning probe microscope in the tapping mode.

NEXAFS experiments were carried out on the U7A NIST/Dow materials characterization end-station at the National Synchrotron Light Source at Brookhaven National Laboratory. The NIST/Dow materials characterization end-station was equipped with a sample holder positioned on a goniometer, which controlled the orientation of the sample with respect to the polarization vector of the X-rays. The partial-electron-yield (PEY) signal was collected using a channeltron electron multiplier with an adjustable entrance grid bias (EGB). All the data reported here are for a grid bias of −150 V. The channeltron PEY detector was positioned at an angle of 45° with respect to the incoming X-ray beam, and in the equatorial plane of the sample chamber. To eliminate the effect of incident beam intensity fluctuations and monochromator absorption features, the FY and PEY signals were normalized by the incident beam intensity obtained from the photo yield of a clean gold grid. A linear pre-edge baseline was subtracted from the normalized spectra, and the edge jump was arbitrarily set to unity

at 320 eV, far above the edge, a procedure that enabled comparison of different NEXAFS spectra for the same number of carbon atoms in the film thickness probed by NEXAFS.[99] Each measurement was taken on a fresh spot of the sample in order to minimize possible beam damage effects.

The X-ray photoelectron spectroscopy measurements were performed using an Axis Ultra XPS system (Kratos) with a monochromatic Al Kα X-ray source (1486.6 eV) operating at 225 W under 7.0×10^{-9} Torr vacuum. Charge compensation was carried out by injection of low-energy electrons into the magnetic lens of the electron spectrometer. The pass energy of the analyzer was set at 40 eV. The energy resolution was set at 0.1 eV with a dwell time of 500 ms. The spectra were analyzed using *CasaXPS* v. 2.1.9 software.

The topography, chemical composition, and water contact angles of the fluorinated surfaces were found to strongly depend on the coating formulation (solvent, solvent mixture, blending the block copolymer with SEBS, relative amounts in the blend), the application technique (spray-coating, drop-casting, spin-coating), and annealing. Figure 10 shows the SFM images of surfaces prepared by spray-coating and drop-casting. Both the surfaces were prepared from 1% (w/w) solution of PS/PI(10/12)F10H9 in TFT and annealed under vacuum at 120 °C for 12 h after vacuum-drying at 60 °C. The spray-coated surfaces showed unexpectedly low water contact angles immediately after spray-coating. However, a gradual increase, toward the values observed in the case of the drop-cast surfaces, was noted after about 1 month. Interestingly, a blend of SABC and SEBS in the formulation for spray-coating resulted in higher water CAs and lower surface roughness. In addition to the use of SEBS in the spray-coating formulation, we found that the use of a 1:1 mixture of TFT and toluene as the solvent gave relatively high water contact angles after the coating and annealing processes (cf. Table 1).

6.4. Biofouling Assays. *Leaching.* Slides were incubated at about 20 °C for 3 days in a 30 L tank of recirculating deionized water. Equilibration with seawater was achieved by transferring the slides to dishes containing artificial seawater 1 h prior to the start of the experiment.

Navicula Settlement and Strength of Attachment. Navicula cultures were prepared in natural seawater supplemented with nutrients, as described in Holland et al.[49] 10 mL of the cell suspension was added to individual compartments of polystyrene culture dishes (Greiner Bio-1), each containing a glass microscope slide, 6 replicates per test surface. After 2 h in the light at 20 °C, the slides were very gently washed in seawater to remove cells which had not attached. The density of cells attached to the surface of 3 replicates was counted on each slide using an image analysis system attached to a fluorescent microscope. Counts were made for 30 fields of view (each 0.17 mm^2) on each slide. The remaining 3 replicates were exposed to a shear stress of 53 Pa in a water channel.[102] The number of cells remaining attached was compared with unexposed control slides (used to determine settlement as above). Data are expressed as percentage removal; 95% error bars are calculated from arcsine-transformed data.

Settlement of Zoospores and Growth and Attachment Strength of Sporelings. Fertile plants of *Ulva linza* were collected from Wembury Beach, England (50°18′ N; 4°02′ W). Zoospores were released and prepared for attachment experiments as described previously.[42] 10 mL of zoospore suspensions (1×10^6 spores per mL) were pipetted into individual compartments of polystyrene culture dishes (Greiner Bio-1) each containing a glass microscope slide, 9 replicates per test surface. The dishes were incubated in the dark at about 20 °C for 1 h. The slides were gently washed in seawater to remove zoospores that had not attached. The density of zoospores was counted as described previously.[23] Sporelings were cultured in enriched seawater medium in individual (10 mL) wells in polystyrene dishes under illuminated conditions on the remaining 6 replicate slides. The medium was refreshed every 2 days and the sporelings cultured for 8 days. After 8 days, sporelings were harvested by scraping with a razor blade from half of each slide. Biomass was determined by extraction of chloro-

phyll.[100,101] To evaluate the strength of attachment of the sporelings, the slides were placed in the flow apparatus and exposed to the flow channel.[102] The slides were positioned such that the area from which the biomass had been removed was at the leading edge with respect to water flow. Biomass was harvested from the remaining half of each slide. Percentage removal was calculated from the before and after flow data. Bars represent the standard error of the mean from arcsine-transformed data.

Acid-washed glass slides and glass slides coated with PDMS were used as standards. The acid-washed glass slides were prepared by washing in Decon detergent before soaking in 1 M hydrochloric acid for 24 h. The PDMS surfaces were prepared using Silastic T-2 mixture from Dow-Corning Corporation, as described in Hoipkemeier−Wilson et al.[23]

References and Notes

(1) Smith, A., Callow, J. A., Eds. *Biological Adhesives*. Springer: New York, 2006 (in press).

(2) Callow, J. A.; Callow, M. E.; Ista, L. K.; Lopez, G. Chaudhury, M. K. The influence of surface energy on the wetting behaviour of the spore adhesive of the marine alga *Ulva linza* (syn. *Enteromorpha linza*). *J. R. Soc. Interface* **2005**, *2*, 319−325.

(3) de Gennes, P.-G.; Brochard-Wyart, F.; Quéré. Capillarity: Deformable Interfaces. In *Capillarity and Wetting Phenomena*; Springer: New York, 2004.

(4) Clarkson, N. The antifouling potential of silicone elastomer polymers. *Recent Adv. Mar. Biotechnol.* **1999**, *3* (Biofilms, Bioadhesion, Corrosion, and Biofouling), 87−108.

(5) Swain, G. W. Redefining Antifouling Coatings. *Prot. Coat. Eur.* **1999**, *4*, 18−25.

(6) Kavanagh, C. J.; Quinn, R. D.; Swain, G. W. Observations of barnacle detachment from silicones using high-speed video. *J. Adhes.* **2005**, *81*, 843−868.

(7) Terlizzi, A.; Conte, E.; Zupo, V.; Mazzella, L. Biological succession on silicone fouling-release surfaces: long-term exposure tests in the harbour of Ischia, Italy. *Biofouling* **2000**, *15*, 327−342.

(8) Brady, R. F., Jr. Properties which influence marine fouling resistance in polymers containing silicon and fluorine. *Prog. Org. Coat.* **1999**, *35*, 31−35.

(9) Baier, R. E. Influence of the initial surface condition of materials on bioadhesion. In *Proceedings of the Third International Congress on Marine Corrosion and Fouling*; Northwestern University Press: Evanston, Illinois, 1973; pp 633−639.

(10) Baier, R. E. Adhesion in the biological environment. *Biomater., Med. Devices, Artif. Organs* **1984−85**, *12*, 133−159.

(11) Dexter, S. C. Influence of substratum critical surface tension on bacterial adhesion − in situ studies. *J. Colloid Interface Sci.* **1979**, *70*, 346−354.

(12) Andrade, J. D., Jr.; Lee, H. B.; Jhon, M. S.; Kim, S. W.; Hibbs, J. B., Jr. Water as a biomaterial. *Trans. Am. Soc. Artif. Intern. Organs* **1973**, *19*, 1−7.

(13) Wu, S. Surface and interfacial tensions of polymers, oligomers, plasticizers, and organic pigments. In *Polymer Handbook*, 3rd ed.; Brandrup, J., Immergut, E. H. Eds.; Wiley: New York, 1989; pp VI-411−VI-449.

(14) Ostuni, E.; Chapman, R. G.; Liang, M. N.; Meluleni, F. P.; Pier, G.; Ingber, D. E.; Whitesides, G. M. Self-assembled monolayers that resist the adsorption of proteins and the adhesion of bacterial and mammalian cells. *Langmuir* **2001**, *17*, 6336−6343.

(15) Andruzzi, L.; Senaratne, W.; Hexemer, A.; Sheets, E. D.; Ilic, B.; Kramer, E. J.; Baird, B.; Ober, C. K. Oligo(ethylene glycol) containing polymer brushes as bioselective surfaces. *Langmuir* **2005**, *21*, 2495−2504.

(16) Senaratne, W.; Andruzzi, L.; Ober, C. K. Self-assembled monolayers and polymer brushes in biotechnology: current applications and future perspectives. *Biomacromolecules* **2005**, *6*, 2427−2448.

(17) Amiji, M.; Park, K. Surface modification of polymeric biomaterials with poly(ethylene oxide), albumin, and heparin for reduced thrombogenicity. *J. Biomater. Sci., Polym. Ed.* **1993**, *4*, 217−234.

(18) Schmidt, D. L.; Brady, R. F., Jr.; Lam, K.; Schmidt, D. C.; Chaudhury, M. J. Contact Angle Hysteresis, Adhesion, and Marine Biofouling. *Langmuir* **2004**, *20*, 2830−2836.

(19) Gudipati, C. S.; Finlay, J. A.; Callow, J. A.; Callow, M. E.; Wooley, K. L. The antifouling and fouling-release performance of hyperbranched fluoropolymer (HBFP)-poly(ethylene glycol) (PEG) composite coatings evaluated by adsorption of biomacromolecules and the green fouling alga *Ulva*. *Langmuir* **2005**, *21*, 3044−3053.

(20) Pullin, R. A.; Nevell, T. G.; Tsibouklis, J. Surface energy characteristics and marine antifouling performance of poly(1*H*,1*H*,2*H*,2*H*-perfluorodecanoyl diitaconate) film structures. *Mater. Lett.* **1999**, *39*, 142−148.

(21) Curtis, A.; Wilkinson, C. New depths in cell behavior: reactions of cells to nanotopography. *Biochem. Soc. Symp.* **1999**, *65*, 15−26.

(22) Granhag, L. M.; Finlay, J. A.; Jonsson, P. R. Callow, J. A.; Callow, M. E. Roughness-dependent removal of settled spores of the green alga *Ulva* exposed to hydrodynamic forces from a water jet. *Biofouling* **2004**, *20*, 117−122.

(23) Hoipkemeier-Wilson, L.; Schumacher, J. F.; Carman, M. L.; Gibson, A. L.; Feinberg, A. W.; Callow, M. E.; Finlay, J. A.; Callow, J. A.; Brennan, A. B. Antifouling potential of lubricious, micro-engineered, PDMS elastomers against zoospores of the green fouling alga *Ulva* (*Enteromorpha*). *Biofouling* **2004**, *20*, 53−63.

(24) Brady, R. F.; Singer, I. L. Mechanical factors favoring release from fouling release coatings. *Biofouling* **2000**, *15*, 73−81.

(25) Berglin, M.; Lönn, N.; Gatenholm P. Coating modulus and barnacle bioadhesion. *Biofouling* **2003**, *19* (Supplement), 63−69.

(26) Stein, J.; Truby, K.; Darkangelo-Wood, C.; Takemori, M.; Vallance, M.; Swain, G.; Kavanagh, C.; Kovach, B.; Schultz, M.; Wiebe, D.; Holm, E.; Montemarano, J.; Wendt, D.; Smith, C.; Meyer, A. Structure−property relationships of silicone biofouling-release coatings: effect of silicone network architecture on pseudobarnacle attachment strengths. *Biofouling* **2003**, *19*, 87−94.

(27) Chaudhury, M. K.; Finlay, J. A.; Chung, J. Y.; Callow, M. E.; Callow, J. A. The influence of elastic modulus and thickness on the release of the soft-fouling green alga *Ulva linza* (syn. *Enteromorpha linza*) from poly(dimethylsiloxane) (PDMS) model networks. *Biofouling* **2005**, *21*, 41−48.

(28) Singer, I. L.; Kohl, J. G.; Patterson, M. Mechanical aspects of silicone coatings for hard foulant control. *Biofouling* **2000**, *16*, 301−309.

(29) Sun, Y.; Guo, S.; Walker, G. C.; Kavanagh, C. J.; Swain, G. W. Surface elastic modulus of barnacle adhesive and release characteristics from silicone surfaces. *Biofouling* **2004**, *20*, 279−289.

(30) Walker, G. C.; Sun, Y.; Guo, S.; Finlay, J. A.; Callow, M. E.; Callow, J. A. Surface mechanical properties of the spore adhesive of the green alga *Ulva*. *J. Adhes.* **2005**, *81*, 1101−1118.

(31) Finlay, J. A.; Callow, M. E.; Schultz, M. P.; Swain, G. W.; Callow, J. A. Adhesion strength of settled spores of the green alga *Enteromorpha*. *Biofouling* **2002**, *18*, 251−256.

(32) Singhvi, R.; Kumar, A.; Lopez, G. P.; Stephanopoulos, G. N.; Wang, D. I. C.; Whitesides, G. M.; Ingber, D. E. Engineering cell shape and function. *Science* **1994**, *264*, 696−698.

(33) Webb, K.; Hlady, V.; Tresco, P. A. Relationships among cell attachment, spreading, cytoskeletal organization, and migration rate for anchorage-dependent cells on model surfaces. *J. Biomed. Mater. Res.* **2000**, *49*, 362−368.

(34) Dewez, J.-L.; Doren, A.; Schneider, Y.-J.; Rouxhet, P. G. Competitive adsorption of proteins: Key of the relationship between substratum surface properties and adhesion of epithelial cells. *Biomaterials* **1999**, *20*, 547−559.

(35) Wu, Y.; Simonovsky, F. I.; Ratner, B. D.; Horbett, T. A. The role of adsorbed fibrinogen in platelet adhesion to polyurethane surfaces: A comparison of surface hydrophobicity, protein adsorption, monoclonal antibody binding, and platelet adhesion. *J. Biomed. Mater. Res.*, *Part A* **2005**, *74A*, 722−738.

(36) Bishop, J. H.; Silva, S. R.; Silva, V. M. A study of microfouling on antifouling coatings using electron microscopy. *J. Oil Colour Chem. Assoc.* **1974**, *57*, 30−35.

(37) Callow, M. E. Algal Biofilms. In *Biofilms: recent advances in their study and control*; Evans, L. V., Ed.; Harwood Scientific: Amsterdam, 2000; Chapter 12, pp 189−209.

(38) Wetherbee, R.; Lind, J. L.; Burke, J.; Quatrano, R. S. The first kiss: establishment and control of initial adhesion by raphid diatoms. *J. Phycol.* **1998**, *34*, 9−15.

(39) Higgins, M. J.; Molino, P.; Mulvaney, P.; Wetherbee, R. Characterizing the structure and nanomechanical properties of the adhesive mucilage that mediates diatom-substratum adhesion and motility. *J. Phycol.* **2003**, *39*, 1181−1193.

(40) Chiovitti, A.; Bacic, A.; Burke, J.; Wetherbee, R. Heterogeneous xylose-rich glycans are associated with extracellular glycoproteins from the biofouling diatom *Craspedostaurosaustralis* (Bacillariophyceae). *Eur. J. Phycol.* **2003**, *38*, 351−360.

(41) Lind, J. L.; Heimann, K.; Miller, E. A.; van Vliet, C.; Hoogenradd, N. J.; Wetherbee, R. Substratum adhesion and gliding in a diatom are mediated by extracellular proteoglycans. *Planta* **1997**, *203*, 213−221.

(42) Callow, M. E.; Callow, J. A.; Pickett-Heaps, J.; Wetherbee, R. Primary adhesion of *Enteromorpha* (Chlorophyta, Ulvales) propagules: quantitative settlement studies and video microscopy. *J. Phycol.* **1997**, *33*, 938−947.

(43) Stanley, M. S.; Callow, M. E.; Callow, J. A. Monoclonal antibodies to adhesive cell coat glycoproteins secreted by zoospores of the green alga *Enteromorpha*. *Planta* **1999**, *210*, 61−71.

(44) Callow, J. A.; Osborne, M. P.; Callow, M. E.; Baker, F.; Donald, A. M. Use of environmental scanning electron microscope to image the spore adhesive of the marine alga *Enteromorpha* in its natural hydrated state. *Colloids Surf., B* **2003**, *27*, 315−321.

(45) Humphrey, A. J.; Finlay, J. A.; Pettit, M. E.; Stanley, M. S.; Callow, J. A. Effect of Ellman's Reagent and dithiothreitol on the curing of the spore adhesive glycoprotein of the green alga *Ulva*. *J. Adhes.* **2005**, *81*, 791−803.

(46) Callow, J. A.; Stanley, M. S.; Wetherbee, R.; Callow, M. E. Cellular and molecular approaches to understanding primary adhesion in *Enteromorpha:* an overview. *Biofouling* **2000**, *16*, 141−150.

(47) Callow, M. E.; Callow, J. A. Substratum location and zoospore behavior in the fouling alga *Enteromorpha*. *Biofouling* **2000**, *15*, 49−56.

(48) Arce, F. T.; Avci, R. Beech, I. B.; Cooksey, K. E.; Wigglesworth-Cooksey, B. Microelastic properties of minimally adhesive surfaces: A comparative study of RTC11™ and Intersleek elastomers. *J. Chem. Phys.* **2003**, *119*, 1671−1682.

(49) Holland, R.; Dugdale, T. M.; Wetherbee, R.; Brennan, A. B.; Finlay, J. A.; Callow, J. A. Adhesion and motility of fouling diatoms on a silicone elastomer. *Biofouling* **2004**, *20*, 323−329.

(50) Finlay, J. A.; Callow, M. E.; Ista, L. K.; Lopez, G. P.; Callow, J. A. The influence of surface wettability on the adhesion strength of settled spores of the green alga *Enteromorpha* and the diatom *Amphora*. *Integr. Comp. Biol.* **2002**, *42*, 1116−1122.

(51) Youngblood, J. P.; Andruzzi, L.; Ober, C. K.; Hexemer, A.; Kramer, E. J.; Callow, J. A.; Finlay, J. A.; Callow, M. E. Coatings based on side-chain ether-linked poly(ethylene glycol) and fluorocarbon polymers for the control of marine biofouling. *Biofouling* **2003**, *19* (Supplement), 91−98.

(52) Becker, K. Exopolysaccharide production and attachment strength of bacteria and diatoms on substrates with different surface tensions. *Microb. Ecol.* **1996**, *32*, 23−33.

(53) PFA (C_2F_4/CF_2=CF$-$OC$_3$F$_7$ copolymer), FEP (perfluoro ethylene/propylene copolymer), and ETFE (C_2H_4/C_2F_4 copolymer).

(54) Wang, J.; Mao, G.; Ober, C. K.; Kramer, E. J. Liquid crystalline, semifluorinated side group block copolymers with stable low energy surfaces: synthesis, liquid crystalline structure, and critical surface tension. *Macromolecules* **1997**, *30*, 1906−1914.

(55) Krishnan, S.; Kwark, Y.-J.; Ober, C. K. Fluorinated polymers: liquid crystalline properties and applications in lithography. *Chem. Rec.* **2004**, *4*, 315−330.

(56) Brady, R. F., Jr. Coming to an unsticky end. *Nature (London)* **1994**, *368*, 16−17.

(57) Schmidt, D. L.; Coburn, C. E.; DeKoven, B. M.; Potter, G. E.; Meyers, G. F.; Fischer, D. A. Water-based nonstick hydrophobic coatings. *Nature (London)* **1994**, *368*, 39−41.

(58) Pittman, A. G. Surface properties of fluoro-carbon polymers. In *Fluoropolymers*; Wall, L. A., Ed.; Wiley-Interscience: New York, 1972; pp 419−449.

(59) Rabolt, J. F.; Russell, R. T.; Twieg, R. J. Structural studies of semifluorinated *n*-alkanes. 1. Synthesis and characterization of F(CF_2)$_n$(CH_2)$_m$H in the solid state. *Macromolecules* **1984**, *17*, 2786−2794.

(60) Genzer, J.; Sivaniah, E.; Kramer, E. J.; Wang, J.; Körner, H.; Xiang, M.; Char, K.; Ober, C. K.; DeKoven, B. M.; Bubeck, R. A.; Chaudhury, M. K.; Sambasivan, S.; Fischer, D. A. The orientation of semifluorinated alkanes attached to polymers at the surface of polymer films. *Macromolecules* **2000**, *33*, 1882−1887.

(61) Chidsey, C. E. D.; Loiacono, D. N. Chemical functionality in self-assembled monolayers: structural and electrochemical properties. *Langmuir* **1990**, *6*, 682−691.

(62) Prime, K. L.; Whitesides, G. M. Adsorption of proteins onto surface containing end-attached oligo(ethylene oxide): a model system using self-assembled monolayers. *J. Am. Chem. Soc.* **1993**, *115*, 10714−10721.

(63) Chan, Y. M.; Schweiss, R.; Werner, C.; Grunze, M. Electrokinetic characterization of oligo- and poly(ethylene glycol)-terminated self-assembled monolayers on gold and glass surfaces. *Langmuir* **2003**, *19*, 7380−7385.

(64) Masuda, Y.; Nakanishi, T. Ion-specific swelling behavior of poly-(ethylene oxide) gel and the correlation to the intrinsic viscosity of the polymjer in salt solutions. *Colloid Polym. Sci.* **2002**, *280*, 547−553.

(65) The polystyrene block imparts solubility to, generally difficult to dissolve, fluorinated polymers in common solvents such as α,α,α-trifluorotoluene, chloroform, THF, or their blends, and prevents leaching of the hydrophilic PEGylated polymer in the marine environment.

(66) Luzinov, I.; Julthongpiput, D.; Tsukruk, V. V. Thermoplastic elastomer monolayers grafted to a functionalized silicon surface. *Macromolecules* **2000**, *33*, 7629−7638.

(67) Luzinov, I.; Julthongpiput, D.; Bloom, P. D.; Sheares, V. V.; Tsukruk, V. V. Bilayer nanocomposite molecular coatings from elastomer/rigid polymers: fabrication, morphology, and micromechanical properties. *Macromol. Symp.* **2001**, *166*, 227−242.

(68) Because the fluorinated block is attached to PS, some styrene units could be detected at the surface. The styrene content decreased upon annealing due to the tendency of the lower surface energy block to be present at the air−polymer interface.

(69) Nadkarni, G.; Garoff, S. An investigation of microscopic aspects of contact-angle hysteresis: pinning of the control line on a single defect. *Europhys. Lett.* **1992**, *20*, 523−528.

(70) From DSC measurements, it is known that a temperature of ca. 98 °C would be required for this to happen (in the absence of a solvent that solvates the side-chains, which is the case during water CA measurements).

(71) Hexemer, A.; Sivaniah, E.; Kramer, E. J.; Xiang, M.; Li, X.; Fischer, D. A.; Ober, C. K. Managing polymer surface structure using surface active block copolymers in block copolymer mixtures. *J. Polym. Sci., Part B: Polym. Phys.* **2004**, *42*, 411−420.

(72) Krishnan, S.; Ober, C. K.; Ayothi, R.; Lin, Q.; Paik, M.; Hexemer, A.; Kramer, E. J.; Fischer, D. Hydrophobic and hydrophilic fluoropolymers as non-adhesive interfaces in marine biofouling. *Polym. Prepr. (Am. Chem. Soc., Div. Polym. Chem.)* **2005**, *46*, 613−614.

(73) Stöhr, J. *NEXAFS Spectroscopy*; Springer-Verlag: New York, 1996; Chapter 7, pp 211−238.

(74) Stöhr, J.; Outka, D. A. Determination of molecular orientations on surfaces from the angular dependence of near-edge x-ray absorption-fine-structure spectra. *Phys. Rev. B* **1987**, *36*, 7891−795.

(75) Outka, D. A.; Stöhr, J.; Rabe, J. P.; Swalen, J. D. The orientation of Langmuir−Blodgett monolayers using NEXAFS. *J. Chem. Phys.* **1988**, *88*, 4076−4087.

(76) Barriet, D.; Lee, R. T. Fluorinated self-assembled monolayers: composition, structure and interfacial properties. *Curr. Opin. Colloid Interface Sci.* **2003**, *8*, 236−242 references therein.

(77) The contribution of different groups to surface energy is in the order $-CH_2 > -CH_3 > -CF_2 > -CF_3$. Hence, to minimize the surface energy, it is desirable to have fewer $-CF_2-$ groups and more $-CF_3$ groups.

(78) Compare with the NEXAFS spectra reported in ref 15.

(79) From the low intensity of 1s $\rightarrow$ π*$_{C=C}$ peak corresponding to polystyrene, in the NEXAFS spectrum of Figure 5, it can be inferred that the SEBS surface is covered mainly by the poly(ethylene-*ran*-butylene) block, whose surface energy is expected to be higher than that of the fluorinated polymer but lower than the surface energy of PEGylated polymer.

(80) Callow, J. A.; Callow, M. E. The *Ulva* spore adhesive system. In *Biological Adhesives*; Smith, A., Callow, J. A. Eds.; Springer: New York, 2006 (In press).

(81) Chiovitti, A.; Dugdale, T. M.; Wetherbee, R. Diatom adhesives: molecular and mechanical properties. In *Biological Adhesives*; Smith, A., Callow, J. A., Eds.; Springer: New York, 2006 (In press).

(82) Baier, R. E.; Meyer, A. E. Surface analysis of fouling-resistant marine coatings. *Biofouling* **1992**, *6*, 165−180.

(83) Gerhart, D. J.; Rittschof, D.; Hooper, I. R.; Eisenman, K.; Meyer, A. E.; Baier, R. E.; Young, C. Rapid and inexpensive quantification of the combined polar components of surface wettability: application to biofouling. *Biofouling* **1992**, *5*, 251−259.

(84) Krishnan, S.; Ramakrishnan, A.; Hexemer, A.; Finlay, J. A.; Sohn, K. E.; Perry, R.; Ober, C. K.; Kramer, E. J.; Callow, M. E.; Callow, J. A.; Fischer, D. A. Anti-biofouling properties of comb-like block copolymers with amphiphilic side-chains. *Langmuir*, in press.

(85) Chung, T. C.; Raate, M.; Berluche, E.; Schulz, D. N. Synthesis of functional hydrocarbon polymers with well-defined molecular structures. *Macromolecules* **1988**, *21*, 1903−1907.

(86) Mao, G.; Wang, J.; Clingman, S. R.; Ober, C. K.; Chen, J. T.; Thomas, E. L. Molecular design, synthesis, and characterization of liquid crystal-coil diblock copolymers with azobenzene side groups. *Macromolecules* **1997**, *30*, 2556−2567.

(87) Lee, K. M.; Han, C. D. Order−disorder transition induced by the hydroxylation of homogeneous polystyrene-*block*-polyisoprene co-polymer. *Macromolecules* **2002**, *35*, 760−769.

(88) Boric acid, B(OH)$_3$, reacts with 1 equiv of NaOH to form sodium borate, NaB(OH)$_4$.

(89) Hopken, J.; Moller, M.; Boileau, S. Self-organization of amphiphilic fluorocarbon-hydrocarbon molecules. I. Synthesis and interfacial activity of allyl ethers. *New Polym. Mater.* **1991**, *2*, 339−356.

(90) Zalipsky, S. Functionalized poly(ethylene glycols) for preparation of biologically relevant conjugates. *Bioconjugate Chem.* **1995**, *6*, 150−165.

(91) Li, J.; Kao, W. J. Synthesis of polyethylene glycol (PEG) derivatives and PEGylated-peptide biopolymer conjugates. *Biomacromolecules* **2003**, *4*, 1055−1067.

(92) Lele, B. S.; Kulkarni, M. G. Single step room-temperature oxidation of polyethylene glycol to poly(oxyethylene)-dicarboxylic acid. *J. Appl. Polym. Sci.* **1998**, *70*, 883−890.

(93) Vigo, T.; Sachinvala, N. D.; Hamed, O. A. Facile preparations of carboxy-endcapped polyethylene oxides (PEO). *Polym. Prepr. (Am. Chem. Soc., Div. Polym. Chem.)* **2002**, *41*, 144−145.

(94) Bobbitt, J. M. Oxoammonium salts. 6. 4-Acetylamino-2,2,6,6-tetramethylpiperidine-1-oxoammonium perchlorate: A stable and convenient reagent for the oxidation of alcohols. Silica gel catalysis. *J. Org. Chem.* **1998**, *63*, 9367−9374.

(95) Imoto, H.; Fujio, A.; Oshima, Y. (Kao Corp., Japan) Preparation of amide ether carboxylic acids as surfactants by oxidation of poly-oxyethylene aminoethyl ethers using nitroxides. Jpn. Kokai Tokkyo Koho 09 151,169, June 10, 1997.

(96) De Luca, L.; Giacomelli, G.; Masala, S.; Porcheddu, A. Trichloro-isocyanuric/TEMPO oxidation of alcohols under mild conditions: A close investigation. *J. Org. Chem.* **2003**, *68*, 4999−5001.

(97) Tashino, Y.; Togo, H. TEMPO-mediated environmentally benign oxidation of primary alcohols to carboxylic acids with poly[4-(diacetoxyiodo)styrene]. *Synlett* **2004**, *11*, 2010−2012.

(98) Hamerton, I. *Recent developments in epoxy resins*; Rapra Review Reports; Rapra Technology: Shawbury, Shropshire, U.K., 1996; Vol. 8, No. 7, Report 91.

(99) Samant, M. G.; Stöhr, J.; Brown, H. R.; Russell, T. P.; Sands, J. M.; Kumar, S. K. NEXAFS studies on the surface orientation of buffed polyimides. *Macromolecules* **1996**, *29*, 8334−8342.

(100) Shoaf, T. W.; Lium, B. S. Improved extraction of chlorophyll *a* and *b* from algae using dimethyl sulphoxide. *Limnol. Oceanogr.* **1976**, *21*, 926−928.

(101) Jeffrey, S. W.; Humphrey, G. F. New spectrophotometric equations for determining chlorophylls *a*, *b*, *c*1 and *c*2 in higher plants, algae and natural phytoplankton. *Biochem. Physiol. Pflanz.* **1975**, *167*, 191−194.

(102) Schultz, M. P.; Finlay, J. A.; Callow, M. E.; Callow, J. E. A turbulent channel flow apparatus for the determination of the adhesion strength of microfouling organisms. *Biofouling* **2000**, *15*, 243−251.